Numerical Modelling of a Large Scale Model Masonry Arch Bridge

NUMERICAL MODELLING OF A LARGE SCALE MODEL MASONRY ARCH BRIDGE

Yi Tao, J.F. Chen, T.J. Stratford & J.Y. Ooi
The University of Edinburgh
Institute for Infrastructure and Environment
School of Engineering
Edinburgh EH9 3JL, Scotland, UK
y.tao@ed.ac.uk, j.f.chen@ed.ac.uk, t.stratford@ed.ac.uk, j.ooi@ed.ac.uk

KEYWORDS: Masonry arch, finite element model, interface element, backfill, model strategies.

ABSTRACT
The behaviour of masonry arch bridges with sand backfills is extremely complex because it involves not only complex materials including sand, brick units and mortar, but also many highly nonlinear interfaces between these materials. This paper summarises several FE modelling techniques for such a complex bridge at different levels of sophistication. Their accuracy and suitability are assessed by comparing their predictions with a large scale model bridge test results.

INTRODUCTION

Masonry arch bridges form a significant part of the transport network from ancient times to modern days. A masonry arch usually fails in a hinge mechanism. The presence of the backfill can significantly affect the arch behaviour in a number of ways. The fill material increases the stability of the arch, either directly by inducing additional compression area in the arch, or indirectly by allowing a distribution of concentrated forces over larger areas. The passive pressure in the structure also provides additional lateral restraint to the arch. This paper presents a summary of an extensive numerical study on the behaviour of masonry arch bridges using four FE models of increasing complexity. The goal was to develop a deeper understanding of the loading and failure mechanism of masonry arch bridges and to select an advanced model suitable for modelling of fibre reinforced polymer (FRP) strengthened masonry arch bridges in a follow-on study.

THE TEST BRIDGE

A two-span one-third scale model masonry arch bridge was tested at the University of Edinburgh to investigate its behaviour with and without FRP strengthening. The two semi-circular single-ring arches were constructed from concrete bricks and cement mortar, with dry sand backfill to a height of 350 mm above the crowns (Figure 1). Initially, each of the spans was individually loaded at its quarter span location (Figure 1) near to collapse to investigate the loading response and to establish a four-hinge mechanism. FRP strengthening was then applied to the two arches, and each of the spans was again tested separately until the failure of the strengthened system. Further details of the experiments can be found in Tao et al. (2011).

FINITE ELEMENT MODELS

Four finite element (FE) models were developed by adopting both macro and micro-macro modelling strategies with various constitutive laws for the masonry arch. The details of each model are summarized in Table 1 accompanied by sketches in Figure 2. The model using the macro modelling strategy is referred as the homogeneous model in this paper because this approach treats the masonry work as a homogeneous isotropic continuum without distinguishing the masonry units, mortar and interfaces between them (Figure 2b). A traction-opening model and a damaged plasticity constitutive model were used to simulate the mortar interface for two meso-interface models in which the units are expanded to

include the mortar layer thickness and the interfaces between units are modelled (Figure 2c). A detailed solid model, which models the actual units and mortar using solid elements (Figure 2d), was finally developed to overcome the shortcomings of both the homogeneous and meso-interface models.

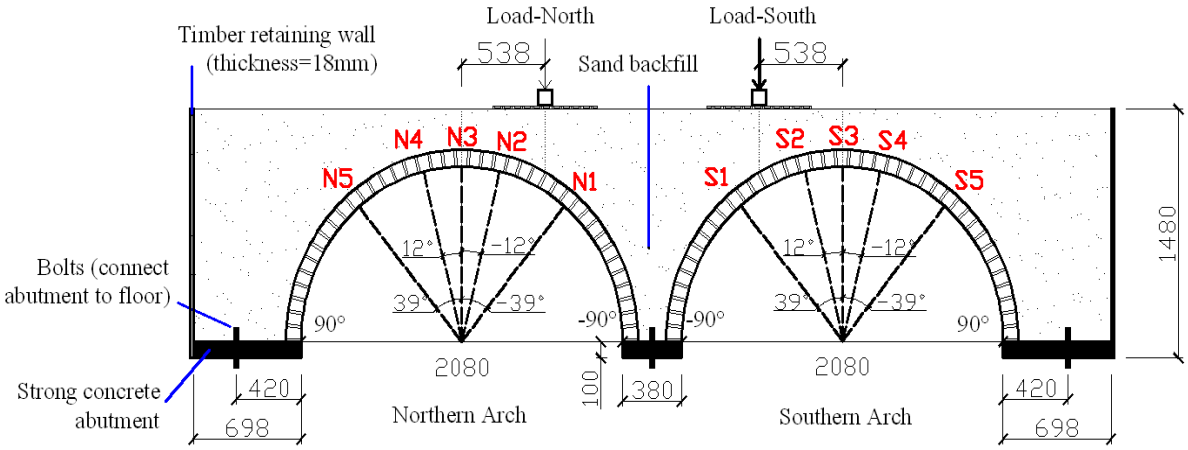

Figure 1: Schematic arch model (dimensions in mm)

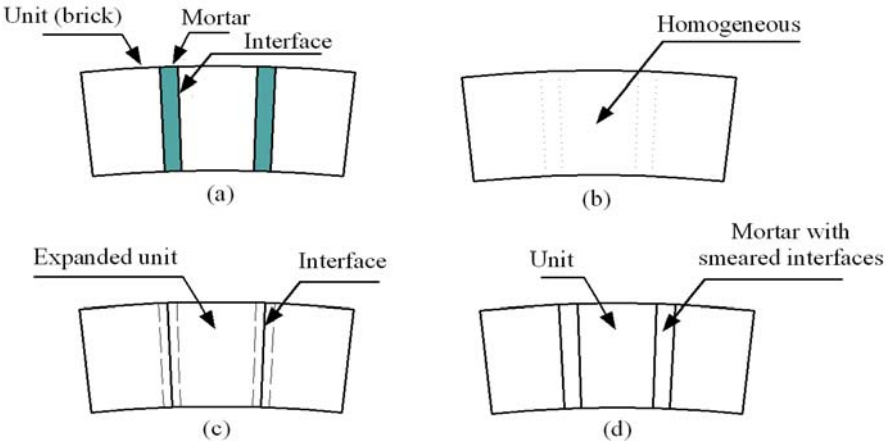

Figure 2: Modelling strategies for masonry arch: (a) local details of masonry work; (b) homogeneous model; (c) meso-interface model; (d) detailed solid model

Table 1: Summary of FE models for the masonry arch bridge

Model		Brick unit		Mortar and interface	
		Unit size	Constitutive model	Representation	Constitutive model
Homogeneous model		NA	Concrete damaged plasticity model	Not modelled explicitly	
Meso interface models	Traction-opening (TO) interface model	Actual size + mortar thickness		Zero thickness interface element	Traction-opening
	Damaged plasticity (DP) interface model				Damaged plasticity
Detailed solid model		Actual size		Solid element with actual mortar thickness	Concrete damaged plasticity

The test arch bridge was modelled as a 2D plane strain problem using the commercial FE software ABAQUS (2007). The whole two-span bridge was modelled because the external load was only applied to a single span in each test so the problem was unsymmetrical. In the FE models, the timber retaining walls and concrete abutments were modelled as linear elastic materials. The sand backfill was modelled using the Mohr-Coulomb plasticity model with a small cohesion c=100Pa and an internal friction angle Φ=33° which was obtained from laboratory tests. The interaction between the sand and the arches, and between the sand and the timber retaining walls were modelled using the contact interface elements in all the FE models with a friction angle between the contact pairs being that of the internal friction angle of sand (i.e. 33°).

The abutments were assumed to be fully restrained in all directions because they were connected to the strong floor using steel bolts as shown in Figure 1. The timber walls were restrained at the top and the bottom laterally using spring boundary elements (Spring 1 element in Abaqus) to model the partial restraint in the test setup. The stiffness of the springs was determined from an analysis of the elastic timber wall (see Tao, 2012). The FE mesh for detailed solid model is shown in Figure 3 and that for other models can be found in Tao (2012). The material properties involved are summarized in Table 2.

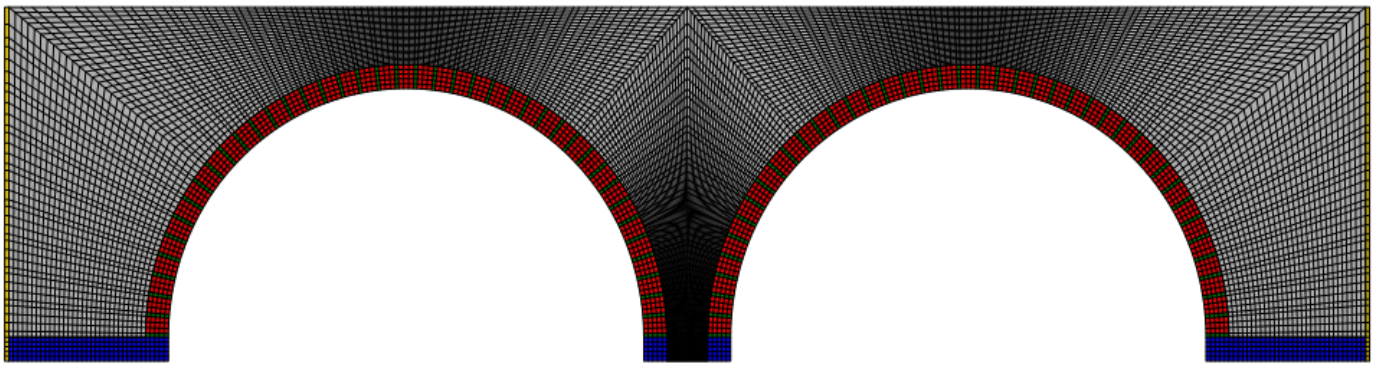

Figure 3: The FE mesh adopted for the detailed solid model

Table 2: Material properties of the masonry arches

	Parameter	Value
Masonry work	Compressive strength f_{cm}	25 MPa
	Young's modulus E_m	16 GPa
Brick Unit	Compressive strength f_{cb}	58.2 MPa
	Tensile strength f_{tb}	4.1 MPa
Mortar interface	Tensile strength f_{ti}^0	0.1 MPa
	Mode-I fracture energy G_{cn}^0	0.066 N/mm
	Initial shear strength τ^0	0.39 MPa
	Mode-II fracture energy G_{ct}^0	0.3 N/mm

Homogeneous model

The critical feature of the homogeneous model is that the weak mortar and brick-mortar interfaces are smeared so that the whole arch is represented by a homogeneous isotropic material (Figure 2(b)). All the components including the arches, timber retaining wall, sand backfill and abutments were modelled using the four node plane strain element with four integration points (CPE4).

The masonry work was modelled using the concrete damaged plasticity (CDP) model available in ABAQUS (2007), because masonry work behaves similar to concrete under both compression and

tension (Lourenço et al. 1995). The uniaxial compressive constitutive behaviour of masonry was modelled using the relationship proposed by Saenz (1964) for plain concrete:

$$\sigma_c = \frac{E_0 \varepsilon_c}{1+\left(\frac{E_0 \varepsilon_p}{\sigma_p}-2\right)\left(\frac{\varepsilon_c}{\varepsilon_p}\right)+\left(\frac{\varepsilon_c}{\varepsilon_p}\right)^2} \quad (1)$$

where σ_c and ε_c are respectively the compressive stress and strain, σ_p and ε_p are the maximum stress and its corresponding strain which are taken to be the compressive strength of the masonry f_{cm} and 0.0022 respectively, and E_0 is 16000MPa. Tensile failure at the mortar-interface is brittle in nature. Therefore, it is difficult to test the full nonlinear behaviour of masonry under tension. In Pluijm (1997) it was shown that the descending branch of masonry under tension can be described by the model developed by Hordijk (1991) for plain concrete:

$$\frac{\sigma_t}{f_t} = \left[1+\left(c_1 \frac{w_t}{w_{cr}}\right)^3\right] e^{\left(-c_2 \frac{w_t}{w_{cr}}\right)} - \frac{w_t}{w_{cr}}\left(1+c_1^3\right)e^{(-c_2)} \quad , \quad w_{cr} = 5.14 \frac{G_F}{f_t} \quad (2)$$

where w_t is the crack opening displacement, w_{cr} is the crack opening displacement at the complete loss of tensile stress, σ_t is the tensile stress, f_t is the tensile strength, and c_1=3.0 and c_2=6.93 are constants. In addition to the material properties of the masonry work listed in Table 2, the tensile strength of the mortar interface was adopted as the tensile strength of the masonry work.

Meso interface models

A critical feature of the two meso-interface models is the use of zero thickness interface elements to simulate the brick to brick interfaces as shown in Figure 2(c), without modelling the actual mortar layer. The thickness of the mortar layer was added to the size of the brick units so that the geometry of the bridge remained unaffected. The brick units were modelled using the CPE4 plane strain element and the interfaces were modelled using the COH2D4 cohesive element available in ABAQUS (2007). The concrete brick units were modelled using the same CDP model as described in the homogeneous model above but with the brick properties listed in Table 2.

Traction-opening interface model

In the traction-opening interface model, the interface was modelled by defining the behaviour of both mode-I and mode-II. A linear softening law was adopted to model the two failure modes as shown in Figure 4. A damage initiation law (Eq. 3) and a damage evolution law (Eq. 4) were used to describe the interaction between the two modes.

$$\max\left\{\frac{\langle\sigma\rangle}{f_{ti}^0}, \frac{\tau}{\tau^0}\right\} = 1 \quad (3)$$

$$\left\{\frac{G_n}{G_{cn}^0}\right\}^2 + \left\{\frac{G_t}{G_{ct}^0}\right\}^2 = 1 \quad (4)$$

where σ and τ are the normal and shear stresses respectively, and G_n and G_t are the work done by the traction and its conjugate relative displacement in the normal and shear directions respectively.

Damaged plasticity interface model

One disadvantage of the traction-opening interface model is that the shear stress does not increase when the interface is under compression as shown in Eq. 3, which does not reflect the actual behaviour of the inter-brick interface. To overcome this drawback, the CDP model available in ABAQUS was used instead here. Although this model was originally developed for concrete, it is appropriate for modelling the mortar interface since it was evolved from the original Drucker-Prager plasticity model by considering the damage effects on the yield conditions and the flow rule. The constitutive law of the mortar interface was thus defined by the compressive and tensile behaviour and a damage law. The compressive strength of the interface was taken as that for the mortar at 12 MPa. The mode-I behaviour in Figure 4(a) was used to model the tensile behaviour including the damage model.

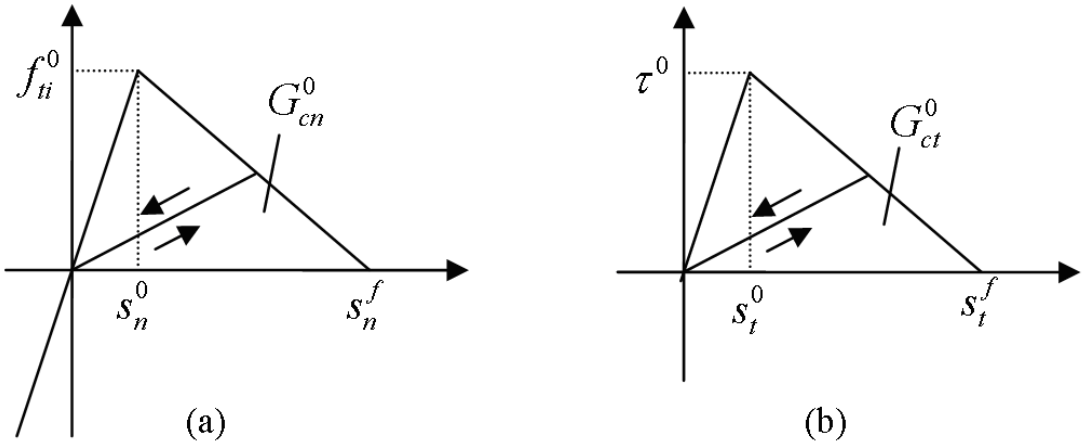

Figure 4: Normal (a) and shear (b) traction-opening displacement relationships of the brick-mortar interface

Detailed solid model

In the above meso-interface models, the mortar layer was neglected. This may not only reduce the accuracy of the models, but also lead to numerical difficulties when modelling more complex systems where the zero thickness interface elements intersect such as in multiple ring arches and in FRP strengthened masonry arch bridges. To overcome these drawbacks, a detailed solid model was developed to represent the mortar interface using the CPE4 solid element with the actual mortar thickness as shown in Figure 2d. The unit-mortar interfaces are smeared into the mortar elements. The mortar was modelled using the CDP model as that in the damaged plasticity interface model, with compressive properties of the mortar and tensile properties of the interfaces. The brick units were modelled in the same way as those in the meso-interface models.

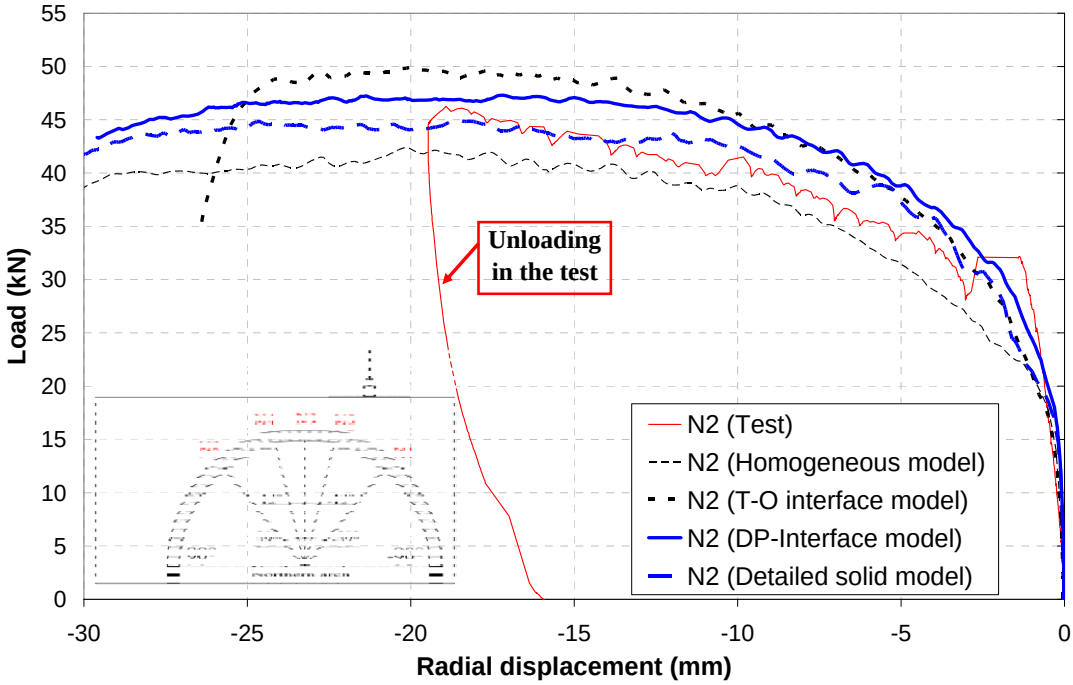

Figure 5: Comparison between FE predictions and experiment

FE PREDICTIONS AND COMPARISON WITH TEST DATA

Figure 5 shows the comparison between the test load-displacement curves and the predictions from the four FE models. The comparison of the four hinge mechanism between the detailed solid model and the test results at the peak load is shown in Figure 6. Note that the location of hinge D reported in Tao *et al.* (2011) was incorrect and it has been corrected here by having carefully checked the photographic records. The loading capacity and locations of the hinges from the four FE models together with that of a mechanism analysis are summarised in Table 3. It is evident that all four models are capable of producing a comparable prediction; however each model has its own characteristics. The homogeneous model was the simplest one which gave the most conservative prediction because the weaker tensile strength was smeared in the whole arch so that cracking can occur inside the bricks rather than at the interfaces in the other models and practice. The traction-opening interface model did not capture the mortar interface behaviour correctly because it did not consider the enhanced shear strength under compression. Although the damaged plasticity interface model delivered a good prediction, it is not suitable for modelling FRP strengthened masonry arch bridge because it can lead to modelling difficulties (Tao 2012). The detailed solid model produced a good agreement with the test and is also suitable for modelling FRP strengthened arch bridges which is one of the purposes of this study.

Table 3: Comparison of main results

		Loading capacity (kN)	Locations of four hinges
Test	North	46.2	-68°, -20°, 20°, 90°
	South	49.7	-68°, -20°, 20°, 90°
Homogeneous model		42.5	-65°, -20°, 29°, 90°
TO interface model		50.0	-65°, -20°, 25°, 90°
DP interface Model		47.5	-65°, -20°, 20°, 90°
Detailed solid model		45.0	-60°, -20°, 20°, 90°
Mechanism analysis		41.9	-58°, -13°, 26°, 90°

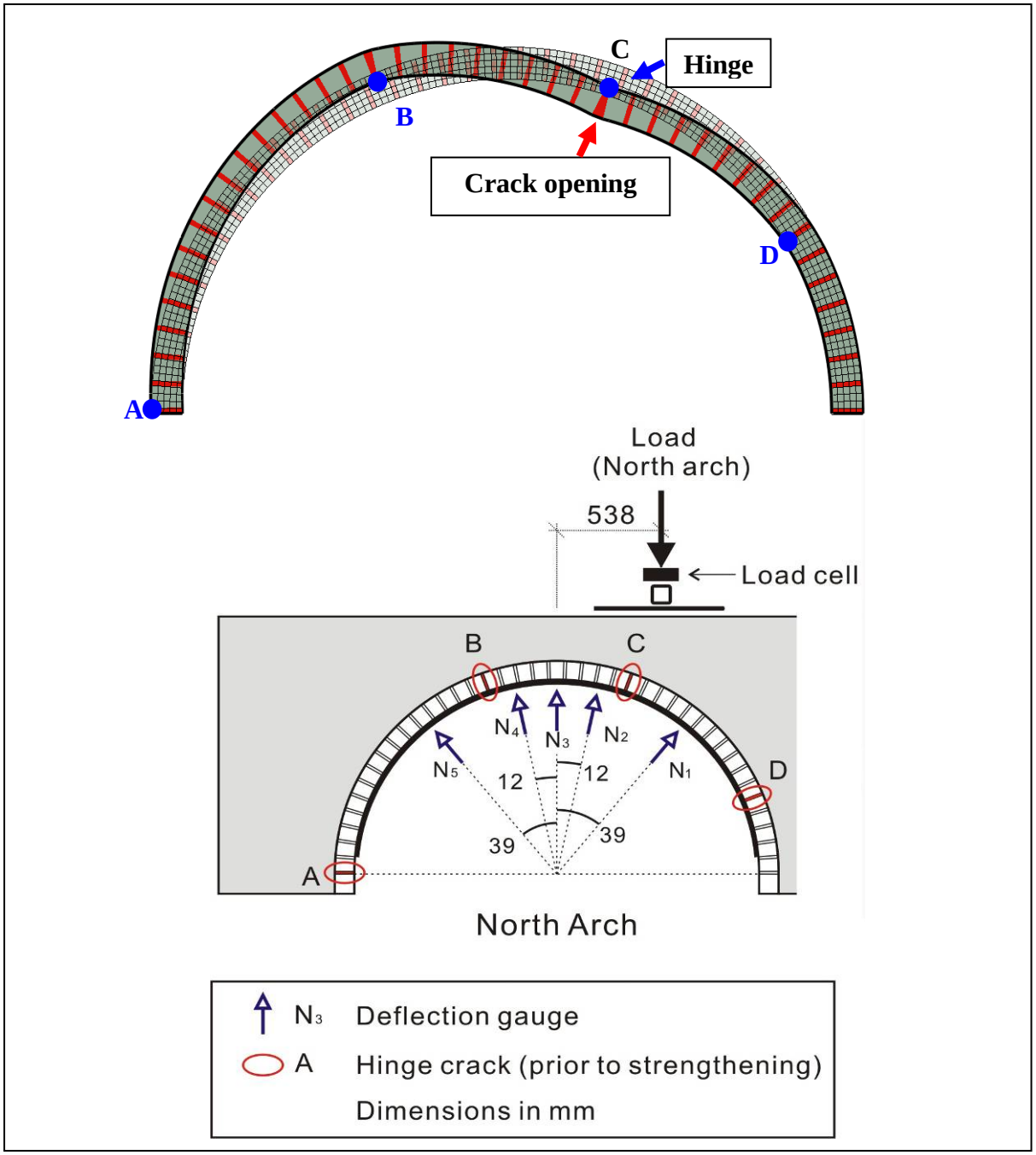

Figure 6: Comparison of the four hinge mechanism between the detailed solid model prediction (upper) and test (lower)

CONCLUSIONS

This paper has presented a numerical study on a masonry arch bridge with sand backfill. The arch bridge was modelled using four different FE models. They all produced reasonably good predictions of the loading behaviour and the associated hinge failure mechanism, with the homogeneous model which does not model the unit-mortar interfaces predicted the lowest loading capacity. As the failure of masonry arch bridges was dominated by the behaviour of the brick-mortar interfaces, an accurate interface model is essential for modelling more complex systems but the interface models pose many numerical challenges. The proposed detailed solid model smears the brick-mortar interfaces into the thin mortar layers, leading to an advantage of being able to accurately modelling the interface behaviour without the need of modelling the actual interfaces and thus avoiding numerical difficulties in complex systems.

REFERENCES

ABAQUS (2007). ABAQUS Analysis user's manual, version 6.7.

Hordijk, D. A. (1991). "Local Approach to Fatigue of Concrete." PhD, Delft University of Technology.

Lourenço, P. B., J.G. Rots and J. Blaauwendraad (1995). "Two Approaches for the Analysis of Masonry Structures: Micro and Macro-Modeling." HERON, 40(4), 313-340.

Pluijm, R. v. d. (1997). "Non-linear Behaviour of Masonry under tension." HERON, 42(1), 25-55.

Saenz, L. P. (1964). "Discussion of equation for the stress-strain curve of concrete-by Desayi, P. and Krishan, S." ACI Journal 61(9), 1229-1235.

Tao, Y., Stratford, T. J. and Chen, J. F. (2011). "Behaviour of a masonry arch bridge repaired using fibre-reinforced polymer composites." *Engineering Structures*, 33(5), 1594-1606.

Tao, Y. (2012). Behaviour of Masonry Arch Bridges Strengthened with FRP. PhD thesis, The University of Edinburgh.